

# Blockade of Rabbit Atrial Sodium Channels by Lidocaine

## Characterization of Continuous and Frequency-Dependent Blocking

F. Roosevelt Gilliam III, C. Frank Starmer, and Augustus O. Grant

Lidocaine block of the cardiac sodium channel is believed to be primarily a function of channel state. For subthreshold potentials, block is limited to the inactivated state, whereas above threshold, block results from the combination of open- and inactivated-state block. Since, in the absence of drug, inactivation develops with time constants that vary from several hundred milliseconds to a few milliseconds as potential is varied from subthreshold to strongly depolarized levels, we would predict a similar voltage dependence of at least a fraction of block. Prior theoretical analyses from our laboratory suggest that there should be a direct parallel between blockade determined with a single pulse and trains of pulses. We tested these predictions by measuring the blockade of sodium current in cultured atrial myocytes during exposure to 80  $\mu$ M lidocaine. We selected two test potentials for most of our studies,  $-80$  mV, which was clearly in the subthreshold range of potentials, and  $-20$  mV, which was close to the peak of the current-voltage curve. With single pulses of increasing duration, block developed with a single exponential time course and with time constants that decreased from  $694 \pm 117$  msec at  $-80$  mV to  $373 \pm 54$  msec at  $-20$  mV. In the absence of drug, inactivation developed with a time constant  $176 \pm 17$  at  $-80$  mV and  $2.9 \pm .5$  msec at  $-20$  mV. Despite the much slower onset of inactivation at  $-80$  mV, no second-order delay in block development was observed. This suggests that at  $-80$  mV block is occurring to a channel conformation that is accessed without delay rather than the classical inactivated state. We compared the kinetics of block during a single continuous pulse with trains of pulses at  $-20$  mV. The rate of block onset was faster during the pulse trains, suggesting an element of "activated state" block. We computed shifts in apparent inactivation from observed steady-state blockade. The computed shifts agree well with those observed, indicating that shifts in apparent inactivation result largely from voltage-sensitive equilibrium blockade. The classical states described in the Hodgkin-Huxley formalism may be too restrictive to fully describe the voltage- and time-dependent block of cardiac sodium channels. (*Circulation Research* 1989;65:723-739)

Lidocaine is believed to exert at least a part of its therapeutic effect by blockade of the transient inward sodium current ( $I_{Na}$ ).<sup>1,2</sup> The kinetics and degree of blockade are strongly dependent on the rate and pattern of stimulation. Blockade is enhanced by depolarization and relieved by rest.<sup>3-6</sup> Because depolarization cycles the chan-

nels between rested, open, and inactivated states, it was natural to assume that block was dependent on channel state. Maximum upstroke velocity ( $V_{max}$ ) experiments have shown that prolongation of the plateau phase of the action potential enhanced blockade by lidocaine.<sup>7</sup> Drugs that shorten the plateau duration antagonize the blocking action of lidocaine.<sup>8</sup> Most sodium channels open very briefly and then undergo inactivation during the first few milliseconds of the action potential or pass directly into the inactivated state. All block was presumed to be inactivated-state block unless it occurred during the first few milliseconds. The inactivated-state block developed slowly over a time frame of several hundred milliseconds. The low efficacy of lidocaine in atrial arrhythmias has been related to the brief duration of the atrial action potential,

From the Departments of Medicine and Computer Science, Duke University Medical Center, Durham, North Carolina.

Supported by grants HL-32994 and HL-32708 from the National Institutes of Health, a Grant-in-Aid and an Established Investigatorship (A.O.G.) from the American Heart Association, and Contract 4414804 from the Office of Naval Research and Grant-in-Aid (F.R.G.) from the American Heart Association, North Carolina Affiliate.

Address for correspondence: Dr. Augustus O. Grant, P.O. Box 3504, Duke University Medical Center, Durham, NC 27710.

Received July 11, 1988; accepted March 8, 1989.

permitting little time for drug interaction with the high affinity inactivated state.<sup>1</sup> The negative shift of the inactivation curve has also been taken as evidence for high affinity for the inactivated state of the sodium channel.<sup>6,9,10</sup>

The direct voltage clamp measurements of  $I_{Na}$  have confirmed and extended the initial observations on  $V_{max}$ . Thus, Bean et al<sup>11</sup> showed that blockade of  $I_{Na}$  by lidocaine in rabbit Purkinje fibers at 17° C required about 1–3 seconds to reach steady state. The experiments of Sanchez-Chapula et al<sup>12</sup> showed a similar slow time dependence. They also showed that block approached an asymptotic value at –10 mV as the level of the test potential was changed. From the magnitude of the lidocaine-induced shift in the apparent inactivation curve, Bean et al calculated  $K_{0.5}$ s of 440 and 10  $\mu$ M for the binding of the drug to the resting and inactivated states of the sodium channels. They could find little evidence for open-state block.

The modulated receptor model accounted for the use-dependent block of sodium channels by postulating state-dependent binding of drugs to the sodium channel.<sup>10,13</sup> To satisfy microscopic reversibility, the apparent inactivation curve of drug-complexed channels was presumed to be shifted to more negative potentials. In general, calculated open- and inactivated-state affinities were several orders of magnitude greater than the rested-state affinity. In contrast, the guarded receptor hypothesis postulated fixed drug-receptor affinity but limited access to the receptor site.<sup>14–16</sup> The activation process was selected as an initial candidate for the guarding function. Channel blockade was modeled as requiring an open m gate, that is, channel passage through the open state. Apparent shifts in inactivation were presumed to result from a binding rate determined by the fraction of activated channels and/or the energy required to move a charged drug in the membrane field. Thus, the state of the channel appeared to be a crucial element in blockade development according to both models.

When some of the published data are examined in detail, there seem to be some inconsistencies between blockade and channel state. In the study of Sanchez-Chapula et al,<sup>12</sup> steady-state inactivation was zero at –50 mV (all channels inactivated) in the presence of 20  $\mu$ M lidocaine. Yet they could demonstrate a further increase of about 30% in the level of block as the test potential was decreased from –50 to +30 mV (data from their Figure 9). They did not find much evidence of open-state block. Bean et al<sup>11</sup> examined the rate of block development by 20  $\mu$ M lidocaine at –69 and +31 mV. Their Figure 9A suggests that block proceeded at about the same rate at both potentials. The former potential was subthreshold, whereas the latter was sufficiently depolarized to activate all the channels.<sup>17</sup> At equilibrium, there was little difference in the level of block between the two potentials despite differences in the initial distribution of channels between the open and

the inactivated states. Using  $V_{max}$  measurements, Matsubara et al<sup>7</sup> could demonstrate no change in the rate of block development as the conditioning potential was varied between –40 and +40 mV.

Recent voltage-clamp experiments in cardiac muscle have demonstrated that in the subthreshold and threshold regions of membrane potential, inactivation proceeds at very different rates. In Purkinje fibers, the inactivation time constant is 90 msec at the subthreshold potentials of –100 mV and 1.8 msec at –20 mV.<sup>18</sup> In cat atrial myocytes, subthreshold inactivation developed with fast and slow time constants of 227 to 57 msec and 1,270 to 289 msec for potentials between –100 and –70 mV, respectively.<sup>19</sup> At +20 mV, the fast and slow time constants were 4 and 20 msec. On the basis of these very different rates of inactivation, one would predict different rates of blockade provided that passage into the inactivated state was rate limiting.

We have examined the rates of development of blockade of the sodium channel by lidocaine at subthreshold and suprathreshold potentials. These rates of development of block have been compared with the rates of development of inactivation at the same potentials. The results show that block may develop in the subthreshold range of membrane potential. This occurrence indicates that the open state was not necessary for block. The slower rate of onset of inactivation in the subthreshold range of membrane potential was paralleled by a slower rate of development of block. This suggests that block occurs in the inactivated state or in a channel conformation having similar voltage dependence.

We have also examined the rate of block development during pulse-train stimulation as the interstimulus interval was varied. The rate of development of block was directly related to the interstimulus interval. The level of steady-state block was also inversely related to interstimulus intervals. Binding affinities determined by continuous and pulse-train stimulation accurately predicted the shift in apparent inactivation and suggested little if any modification of gating kinetics in drug-complexed channels.

## Materials and Methods

### Cell Preparation

The experiments were performed on isolated rabbit atrial myocytes. The methods of heart isolation and perfusion by the Langendorff technique were similar to those previously described from our laboratory.<sup>20</sup> As far as possible, sterile technique was used, and all solutions were maintained at 37° C throughout the isolation procedure. All isolation steps involving the use of “Kraft Bruhe” solution were omitted. After 40 minutes of perfusion of the heart with enzyme-containing solution, the atria were excised and placed in a preheated petri dish containing gassed  $Ca^{2+}$ -free Krebs-Henseleit (K-H) solution with 10% fetal bovine

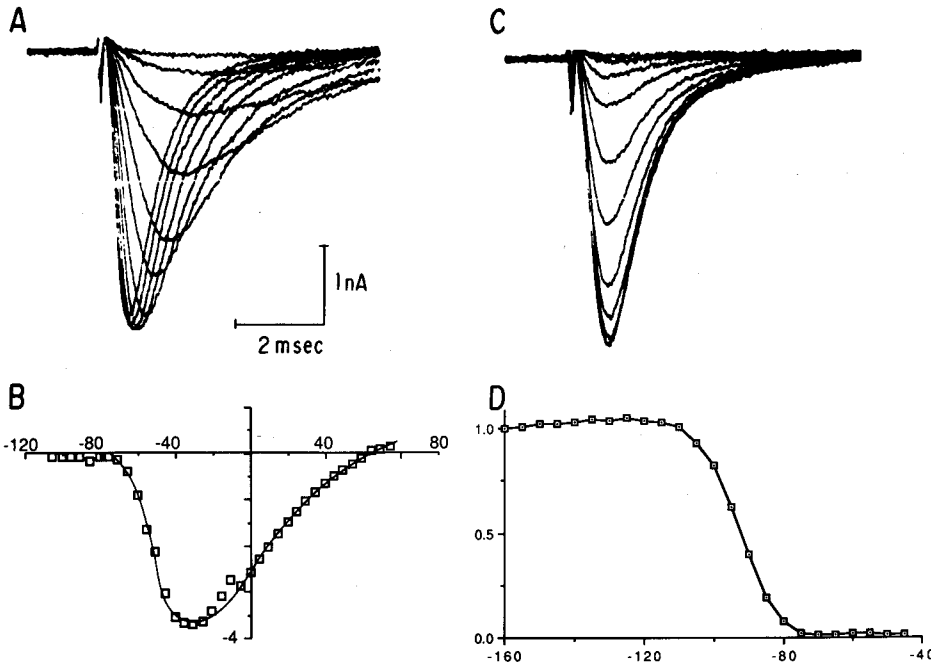


FIGURE 1. Tracings and plots showing characteristics of sodium current in rabbit atrial myocytes. Panel A shows currents recorded in an atrial myocyte under voltage clamp. The currents illustrated are from the negative limb of the current-voltage ( $I$ - $V$ ) curve only. They were photographed from the screen of the oscilloscope. Currents were filtered at 20 kHz before display. The holding potential was  $-120$  mV. Current and time calibration are shown on the lower right corner of the panel. All the points ( $\square$ ) obtained for the  $I$ - $V$  curve are summarized in panel B. Currents during inactivation curve determination are shown in panel C. From a holding potential of  $-120$  mV, 1-sec prepulses were applied to various prepotentials followed by a test pulse to  $-20$  mV. There is no crossover of the currents as their size changes with holding potential and the peak occurs at about the same time. The normalized steady-state inactivation curve is shown in panel D. The continuous line is drawn to connect the data points ( $\blacksquare$ ). The temperature was  $15^\circ$  C.

serum, penicillin G 1 unit/ml, and streptomycin 0.5 unit/ml. The atria were minced into 2–4-mm segments. The segments were transferred to 5 ml serum free K-H medium containing 2.5 mg elastase (Sigma, St. Louis, Missouri).<sup>21</sup> They were then incubated in a water bath at  $37^\circ$  C for 15–30 minutes. A small aliquot was checked every 5 minutes to monitor the progress of the dissociation. For the final dissociation, the tissue segments in K-H medium were placed on an orbital shaker for 5 minutes. The isolated myocytes were separated from the undissociated segments by filtration. They were then plated onto  $18 \times 18$ -mm laminin-coated coverslips ( $4 \mu\text{g}$  laminin/well) and placed in medium containing Dulbecco minimal essential medium (DMEM) and Hams F12 in a 1:1 ratio, 10% fetal bovine serum, 1 unit/ml penicillin, and 0.5 unit/ml streptomycin. The cell cultures were kept at  $37^\circ$  C in a humidified 5% enriched  $\text{CO}_2$  atmosphere until ready for use. In culture, the rod-like atrial cells assumed a spherical shape after 24–48 hours. The cells were used after 2–5 days in culture.

### Solutions

The K-H solution used in the cell isolation procedure had the following composition (mM): NaCl 118.2,  $\text{CaCl}_2$  2.7, KCl 4.7,  $\text{MgSO}_4 \cdot 7\text{H}_2\text{O}$  1.2,  $\text{NaHCO}_3$  25,  $\text{NaH}_2\text{PO}_4$  1.2, and glucose 11. The solution was gassed with 95%  $\text{O}_2$ -5%  $\text{CO}_2$ . "Calcium free" K-H solution had no added calcium. The enzyme perfusate contained 180 units/ml collagenase (Worthington Biochemical, Freehold, New Jersey) and 10 mg/100 ml hyaluronidase (Sigma). DMEM and Hams F12 were obtained from GIBCO Scientific (Grand Island, New York).

For whole-cell recording, the micropipettes were filled with the following solution (mM): CsCl 60, CsF 60,  $\text{MgCl}_2$  5,  $\text{K}_2$  (ATP) 5,  $\text{KH}_2\text{PO}_4$  1, EGTA 5, glucose 5, and HEPES 5. The pH was adjusted to pH 7.3 with CsOH or HF. The external solution was prepared by mixing a 100% and 0% external sodium solution to give the desired external sodium concentration, usually 75 mM. The 100% sodium external solution had the following composition (mM): NaCl 150,  $\text{MgCl}_2$  1, KCl 5,  $\text{CaCl}_2$  1.5, glucose

5, and HEPES 5. The pH was adjusted to 7.4 with NaOH or HCl. For the 0% external sodium solution, CsCl replaced NaCl, and pH was adjusted to 7.4 with CsOH or HCl.

### Recording Techniques

Micropipettes were pulled from 1.5 mm o.d. borosilicate glass (N-51A Drummond Scientific, Broomall, Pennsylvania) with a vertical puller (model 750, David Kopf, Tujunga, California). Micropipettes were coated with Sylgard 184 (Dow Corning, Midland, Michigan). When filled with internal solution, the microelectrodes had resistances of 400–1,100 K $\Omega$ . A patch-clamp amplifier (model EPC 7, List Electronics, Darmstadt, FRG) was used to measure whole-cell currents. The microelectrode was coupled to the amplifier head stage with an Ag/AgCl wire coated with Teflon up to its tip (In Vivo Metric Systems, Healdsburg, California). Whole-cell currents were recorded on an analogue tape recorder (model 4DS, Racal Instruments, Vienna, Virginia) at 30 in/sec, "wideband width 1." This gave an effective bandwidth of DC–20 KHz. Command pulses were provided by an IBM-XT microcomputer and TL-1 interface (Axon Instruments, Burlingame, California). The voltage-clamp protocols were loaded on the fixed disk drive and run as a batch file after stable voltage clamp conditions had been achieved.

On the day of the studies, the serum-containing culture medium was replaced by serum-free medium. A coverslip containing cells was fixed to the base of a recording chamber. The latter was mounted on an inverted microscope (Nikon Diaphot, Nikon, Garden City, New York). The recording chamber and the perfusing solutions were kept at 15° C with a peltier-based system (TS-4 Thermal Microscope Stage, Sortek, Clifton, New Jersey). Some of our initial studies were performed at 18° C. A giga-seal was obtained as outlined by Hamill et al.<sup>22</sup> After a seal of at least 1 G $\Omega$  was obtained, the capacity of the electrode and amplifier input was nulled, then the membrane patch was ruptured. The additional capacity transient was nulled, and the series resistance compensated simultaneously. We could compensate for 50–90% of the series resistance. A current-voltage (I-V) relation was performed by applying depolarizing voltage pulses of increasing amplitude from the holding potential (protocol detailed below). If any threshold phenomenon was observed in negative limb of the I-V curve, the experiment was abandoned. From the peak of the I-V, we estimated the voltage error resulting from uncompensated series resistance. We proceeded with the experiment if the voltage error was less than 3.5 mV.

### Experimental Protocols

Throughout these experiments, the holding potential was fixed at –120 mV. This holding potential was sufficiently negative to remove resting inacti-

vation in the absence of drugs. The I-V relation was first determined with 40-msec pulses of increasing amplitude applied at 1,500-msec intervals. The pulse amplitude was incremented in 5-mV steps from a potential of –110 to +80 mV. The steady-state inactivation curve was determined by the application of 1-sec prepulses to potentials from –160 to –40 mV. A test pulse of 10-msec duration to –20 mV followed. The potential was incremented 5 mV between each prepulse. We then performed one or more of the pulse protocols described below, followed by exposure to 80  $\mu$ M lidocaine for 15 minutes. The protocols were then repeated. In some experiments, we attempted a washout.

*Development of block with single pulses.* The rate of development of block was determined by application of prepulses of increasing duration to a conditioning potential  $V_p$ . In our initial experiments we used prepulse duration of 50 msec to 3 seconds. Prepulse duration was increased in 50-msec increments from 50 to 500 msec, in 100-msec increments from 500 to 1,000 msec, and in 200-msec increments thereafter to 3 seconds. In three experiments we also used an initial duration of 10 msec, which was increased to 50 msec in 10-msec increments. Another three experiments involved an initial prepulse of one msec, which was incremented by 1 msec to 10 msec and by 5 msec to 40 msec; 20-msec increments from 60 to 100 msec; 100-msec increments from 200 to 400 msec; 200-msec increments from 600 to 1,500 msec; and 500-msec increments from 2,000 to 3,000 msec. The conditioning prepulse was followed by a return to the holding potential for 500 msec, then a test pulse of 10-msec duration to –20 mV.<sup>12</sup> There was a recovery period of 10 seconds between the test pulse and the subsequent conditioning pulse. We selected two prepulse potentials for detailed study. One potential, –80 mV was clearly in the subthreshold range for channel activation; the other potential, –20 mV, was in the neighborhood of peak of the I-V curve. Additional experiments were also performed at conditioning potentials of –70 mV and –40 mV. We measured the rate of development of inactivation in the absence of drugs at –80, –70, –40, and –20 mV. At –80 mV, prepulses of 10-msec to 2-second duration were applied, followed immediately by a test pulse to –20 mV. The prepulse duration was increased in 10-msec increments for prepulse durations of 10–100 msec, in 20-msec increments for prepulse durations 100–200 msec, in 50-msec increments for prepulse durations 200–400 msec, and in 200-msec increments for prepulse durations 400 msec–2 seconds. For inactivation measurements at –20 mV, prepulses of 1–20-msec duration were followed by test clamps to –60 mV, and the peak tails at –60 mV were used as a measure of sodium current availability. For prepulses of 1–10 msec, the increments in duration were 1 msec; for prepulses of 10–20 msec, increments in duration were 2 msec. An additional measure of inactivation at –20 mV placed prepulses

of 1–30-msec duration to  $-20$  mV, followed by test clamps to 0 mV; the peak current at 0 mV was used as a measure of sodium current availability. Pre-pulses were incremented by 1 msec from 1 to 10 msec and then in 5-msec increments to 30 msec.

**Development of block with pulse train stimulation.** We used a number of pulse stimulation protocols to examine block development in the subthreshold and threshold levels of membrane potential. We compared the level of block produced by a pulse train with a single pulse of the same overall duration.<sup>7</sup> The train consisted of fifteen 50-msec pulses with 100 msec between the pulses, followed by a recovery interval of 500 msec and a test to  $-20$  mV. The block was compared with that developed during single pulses of 2.15 sec with the same test pulse paradigm. We investigated the contribution of stimulus duration on the development of block. We compared levels of block after 2-, 10-, 20-, and 50-msec pulses in trains of 30 pulses.

We analyzed the dependence of block development on membrane potential and stimulus frequency. To determine the dependence on membrane potential, trains of fifteen 50-msec pulses with an interpulse interval of 100 msec were followed by a recovery interval of 100 msec and a test to  $-20$  mV. The voltage level during the pulse was increased from  $-85$  to  $-40$  mV. In the final series of experiments, we examined the effects of stimulus frequency on blockade. Trains of twenty-five 50-msec pulses were applied at interpulse intervals of 150, 250, 350, 450, 550, and 650 msec.

#### Data Analysis

Currents were filtered at 5 KHz with an 8-pole Bessel filter (model 902, LPF Frequency Devices, Haverhill, Massachusetts). They were digitized at 20 KHz and stored on a fixed disk drive. Current tails were digitized at 40 KHz. Peak values of current were measured with custom software written in "C" programming language. Exponentials were fitted to the data describing the development of block and inactivation using a Marquardt routine or the Gauss-Newton method.<sup>23</sup> We fitted one then two exponentials to the data set. From the residual error, we calculated an  $F$  statistic. We accepted the two-exponential fit if it provided a better fit with a significance of less than 0.05.

### Results

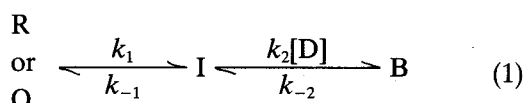
#### Characteristics of the Sodium Current in Cultured Atrial Myocytes

We shall briefly outline the properties of the sodium currents measured in cultured atrial myocytes. Experiments were performed on spherical cells only. In 12 myocytes, cell capacitance average  $28 \pm 6$  pF. This value is 32% of that reported for ordinary atrial cells and 18% of that reported for cells of the crista terminalis.<sup>19,24</sup> The cultured atrial cells are free of T tubules.<sup>25</sup> With the favorable cell

size and shape and the use of low-resistance microelectrodes, a fast voltage clamp can be achieved with the capacitive transient lasting 50–150  $\mu$ sec without series resistance compensation. We were able to compensate for 50–90% of the series resistance with further reduction of the duration of the transient. The threshold potential was  $-64 \pm 9$  mV, and the I-V curve peaked at  $-35 \pm 7$  mV. The mean peak current density was 0.125 nA/pF. This value is comparable with that observed in other atrial myocytes.<sup>19,24</sup> The steady-state inactivation curve could be fitted with a Boltzmann function. Half maximal inactivation ( $V_h$ ) was observed at  $-91 \pm 6$  mV. This value is clearly more negative than in tissue preparations but is typical for isolated dialyzed cells at low temperature (e.g., Reference 26). We could not identify a true reversal of transient current. The measured current approached the voltage axis asymptotically. This is consistent with the lack of sodium ions in the pipette solution. Characteristics of the I-V and inactivation curves from a typical experiment are summarized in Figure 1. The negative limb of the I-V curve spanned a 40-mV range. There was no crossover of current traces as the holding potential was varied during steady-state inactivation measurements. These characteristics suggest that good voltage control was achieved.

#### Development of Block With Single Pulses

Figure 2 illustrates the rate of development of block in response to a single pulse of increasing duration. In the absence of drug there was a slight decrease in peak current for  $-20$ -mV conditioning pulses beyond 2 seconds.<sup>12</sup> During exposure to 80  $\mu$ M lidocaine, peak inward current declined as prepulse duration was increased. For a single exponential fit to the curve describing block at  $-80$  mV, the mean square error was 0.0033 nA<sup>2</sup>. For the double exponential fit, the mean square error was 0.0032 nA<sup>2</sup>. This did not represent an improvement in fit ( $p > 0.05$ ). Further, the 95% confidence interval of one of the coefficients of the double exponential fit included zero. Therefore, we used a single exponential to describe the onset of block. The conclusions from the fitting procedure for the data at  $-20$  mV were similar; one exponential provided an adequate fit. The time constants for the development of block, in this experiment, were 559 msec at  $-80$  mV and 385 msec at  $-20$  mV. The apparent steady-state level of block was 78 and 86% at  $-80$  and  $-20$  mV, respectively. In this experiment steady state inactivation was approximately zero at both  $-80$  and  $-20$  mV. Analysis of the data was approached with the following scheme (scheme 1) for blockade development during the prepulse:



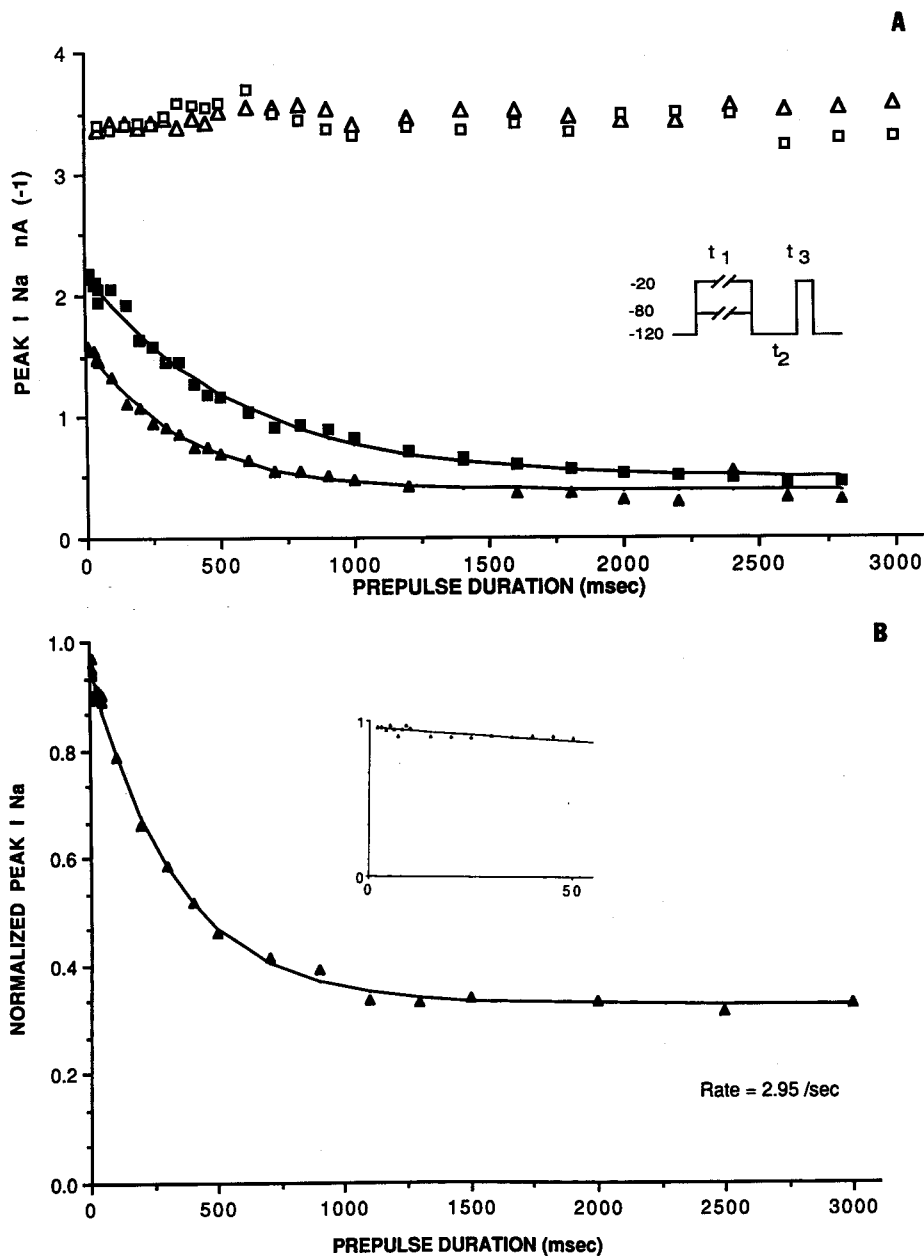


FIGURE 2. Graphs showing block of the sodium current during application of single pulses. Panel A: Peak sodium currents (nA) are plotted on the ordinate; time (msec) is plotted on the abscissa. The pulse paradigm is shown in the inset. From a holding potential of  $-120$  mV, conditioning voltage steps of increasing duration are applied to  $-80$  (■, □) or  $-20$  mV (▲, △). The empty symbols show the control responses; the filled symbols show the responses during exposure to  $80$   $\mu$ M lidocaine. The continuous lines are single exponential fits to the data points during drug exposure. The time constants for the development of block were  $559$  and  $385$  msec at  $-80$  and  $-20$  mV, respectively. The steady-state levels of block were  $77$  and  $86\%$ . The temperature was  $15^\circ$  C. Panel B: This panel shows the results from another cell during exposure to  $80$   $\mu$ M lidocaine. The initial prepulse duration was initially  $1$  msec. The prepulse duration was incremented by  $1$ -msec steps to  $10$  msec, by  $5$ -msec steps to  $40$  msec, and by  $20$ -msec steps to  $100$  msec. Thereafter, the prepulse duration was increased by  $100$ -,  $200$ -, and  $500$ -msec increments. The test potential was  $-20$  mV. The normalized currents were plotted on the ordinate (peak value of current was  $-4.0$  nA under drug-free conditions; current during lidocaine exposure normalized to that during the drug-free period). The prepulse duration was plotted on the abscissa. The abscissa has been expanded in the inset to show the points (▲) for prepulse durations of  $1$ – $50$  msec. The continuous line in the figure and inset are the best-fit single exponential to the data points.

TABLE 1. Rates of Development of Block and of Inactivation

Experiment number	$\tau$ (-80 mV)	Percentage block	$\tau$ (-70 mV)	Percentage block	$\tau$ (-40 mV)	Percentage block	$\tau$ (-20 mV)	Percentage block
<i>A. Rate of development of block during exposure to 80 <math>\mu</math>M lidocaine</i>								
419	909	71	769	79	...	...	435	74
211a	...	...	704	79	555	81	...	...
211b	...	...	520	93	397	90	...	...
208	670	71	...	...	...	...	400	75
128	559	77	...	...	...	...	385	86
125a	697	73	...	...	...	...	437	73
125b	637	74	...	...	...	...	379	75
908b	...	...	...	...	...	...	266	71
908c	...	...	...	...	...	...	322	71
908d	...	...	...	...	...	...	359	67
Mean $\pm$ SD	694 $\pm$ 117	73 $\pm$ 0.2	664 $\pm$ 105	84 $\pm$ 7	467	86	373 $\pm$ 54	74 $\pm$ 5
<i>B. Rate of development of inactivation in the absence of drug</i>								
201	148	...	...	...	...	...	2.79	...
202a	184	...	...	...	...	...	3.14	...
202b	179	...	...	...	...	...	2.86	...
202c	194	...	...	...	...	...	2.33	...
202d	...	...	...	...	...	...	3.14	...
926	...	...	58.6	...	...	...	3.51	...
927a	...	...	...	...	...	...	1.63	...
927b	...	...	91.8	...	6.97	...	2.30	...
1004A	...	...	132	...	13.2	...	3.13	...
1004B	...	...	...	...	7.45	...	3.55	...
Mean $\pm$ SD	176 $\pm$ 17	...	94	...	9	...	2.9 $\pm$ 0.5	...

$\tau$ , time constant of block development or inactivation.

The percentage block was calculated using the largest peak inward current observed during drug exposure.

where R, O, I, and B represent the resting, open, inactivated, and blocked states, respectively, of the channels and  $[D]$  represents the drug concentration.  $k_i$  denotes the first order rate constant for the transition between the indicated states. The slow development of block as prepulse duration increases is presumed to result from the initial passage of channels into the inactivated state followed by blockade by lidocaine.<sup>7</sup> When the rate of transition to the inactivated state is of the similar order of magnitude to the blocking process, block should develop as a double exponential (assuming that drug actually binds to the I state). In three experiments, we added five data points with prepulses of duration 10–50 msec, and in an additional three experiments, prepulses starting with a duration of 1 msec were performed in an attempt to identify an initial fast component of block if one indeed existed (Figure 2B). Single exponentials provided an adequate fit to the data in these experiments. We therefore conclude that block develops slowly with a single exponential time course. The differences in the zero intercept current level for the curves at –20 and –80 mV during lidocaine exposure suggest an element of activated-state blockade occurring at very early times.<sup>7</sup> This was confirmed with trains of 2-msec pulses, which are described later.

We have summarized the results of all of these experiments in Table 1. At a given potential, the rate of block was variable between preparations. However, in all preparations, block developed more rapidly at the more depolarized potential. In principle, this was the type of voltage dependence that would be predicted from scheme 1 above. However, even at depolarized potentials where the transition to the inactivated state is rapid, drug binding remains a slow process.

In order to gain more insight into the relation between the rate of development of inactivation and of block, the rate of development of inactivation was measured at –80 mV and at –20 mV. Figure 3 illustrates the results of one experiment. We used a standard two-pulse protocol for the –80 mV voltage level, and inactivation developed with a time constant of 176 msec. The rate of inactivation at –20 mV was determined from the peak of the tail currents after a step to 0 mV or on return to –60 mV. We chose –60 mV because the tails were slower at this potential compared with their time course at the holding potential of –120 mV.<sup>19</sup> The inactivation time constant declined to 2.9 msec at –20 mV. At both potentials, a single exponential provided an adequate fit. This is at variance with the results of Follmer et al,<sup>19</sup> who observed a double

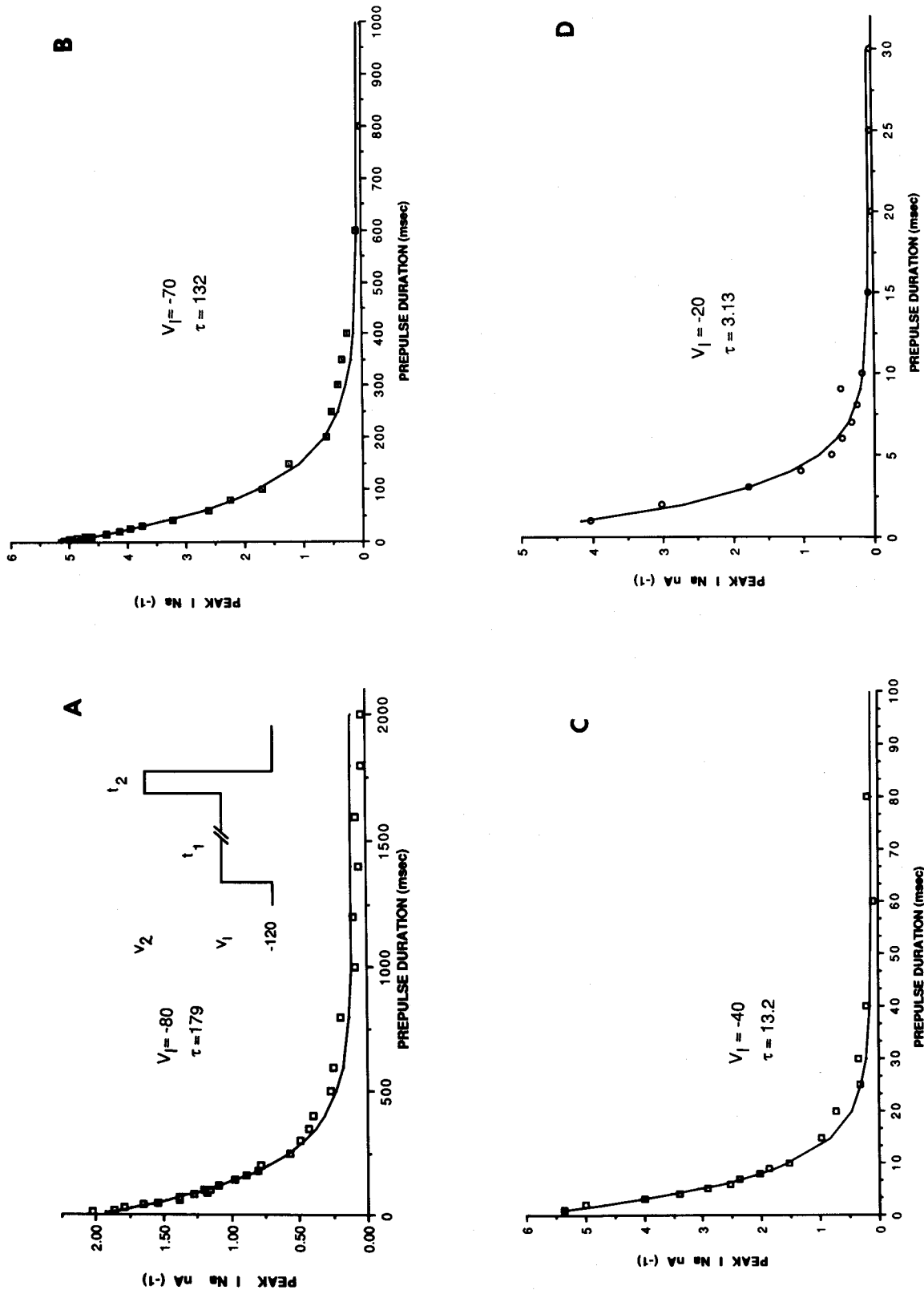


FIGURE 3. Graphs showing the rate of development of inactivation in the absence of drug. In each panel, peak sodium currents are shown on the ordinate, and prepulse duration is shown on the abscissa. The continuous line is single-exponential least-squares fit to the data points. Panel A shows the measurement at  $-80$  mV. From a holding potential of  $-120$  mV, conditioning pulses of increasing duration ( $t_1$ ) are applied at  $-80$  mV, followed immediately by a test pulse of 10-msec duration ( $t_2$ ) to  $-20$  mV. Similar measurements are shown with the prepotential ( $V_1$ ) set at  $-70$  mV in panel B and at  $-40$  mV in panel C. The prepotential was  $-20$  mV in panel D, and the test potential  $V_2$  was 0 mV.  $\tau$ , time constant of inactivation.



exponential in cat atrial myocytes. However, there is a difference in our protocol compared with theirs. We omitted the 3-msec return to the holding potential because our preliminary experiments indicated that some recovery from inactivation occurred during this period. The results of studies at all four potentials are summarized in Table 1B. The decrease in the time constant for the development of block between  $-80$  and  $-20$  mV is of the same order as the decrease in the time constant of development of inactivation at these potentials.

The measurement of the kinetics of block development and of inactivation at the same potential permit an initial quantitative analysis of scheme 1. The matrix for the transition between the various states is given by:

$$M = \begin{pmatrix} -k_1 & k_{-1} & 0 \\ k_1 & -(k_{-1} + k_2D) & k_{-2} \\ 0 & k_2D & -k_{-2} \end{pmatrix} \quad (2)$$

M has two eigenvalues  $\lambda_1$  and  $\lambda_2$  given by:

$$\lambda_{1,2} = [C_2 \pm \sqrt{C_2^2 - 4C_1}] / 2 \quad (3)$$

where  $C_1 = [k_1k_2D + k_1k_{-2} + k_{-1}k_{-2}]$  (4)

$$C_2 = [k_1 + k_{-1} + k_2D + k_{-2}] \quad (5)$$

The equation describing block would be of the following form:

$$B(t) = F_o + F_1 \exp(-\lambda_1 t) + F_2 \exp(-\lambda_2 t) \quad (6)$$

where  $F_o$ ,  $F_1$ , and  $F_2$  are constant. In principle, block according to scheme 1 should develop as a double exponential.

Single channel analysis in neuronal preparations suggests that at markedly depolarized potentials, resting and open channels inactivate at similar rates.<sup>27</sup> Therefore at  $-20$  mV the R and the O states can be treated as equivalent as far as their passage to the inactivated state is concerned. At  $-20$  mV inactivation is essentially irreversible, that is,  $k_{-1} = 0$ . Applying this limiting value to equations 3–6,

$$B(t)_{-20} = F_o + F_1 \exp(-k_1 t) + F_2 \exp(-(k_2 + k_2D)t) \quad (7)$$

That is, block develops as a double exponential with rate constants given by the inactivation rate constant for  $-20$  mV ( $k_1$ ) and a second blocking rate constant ( $k_{-2} + k_2D$ ). At  $-20$  mV, the mean inactivation rate constant in four experiments was 0.36/msec. This is too fast a rate constant to resolve with realistic protocols in the presence of drug. Hence the single exponential time course of block measured experimentally is consistent with scheme 1.

In contrast to the case at  $-20$  mV, the mean rate constant for the development of inactivation at  $-80$  mV was 0.006/msec. The mean block rate constant at  $-80$  mV was 0.0014/msec. Provided that the holding potential was negative enough to force most channels into the resting state, the slower inactivation

at  $-80$  mV should introduce a second-order delay in the development of block. The holding potential of  $-120$  mV is enough to place most channels in the R state. Therefore  $F_1$  and  $F_2$  of Equation 6 should be nonzero. At a 95% level of confidence, we could not identify a second exponential component to the blocking process consistent with this delay. The experiments are consistent with one  $F \sim 0$ .

Therefore, the experiments raise the possibility that block could be occurring in a simple voltage-dependent manner derived from the voltage-dependent channel conformation, but with the binding channel configuration having a similar voltage dependence to that of inactivation, for instance, a preinactivated state. Prior discussions of models of channel blockade already raised this possibility.<sup>1,28</sup>

### Block During Pulse-Train Stimulation

In principle, it could be the transition from the resting to the depolarized potential and/or the sojourn at the depolarized potential that could be important in the development of block. Indeed with quinidine, both  $V_{max}$  and voltage-clamp experiments suggest this to be the case.<sup>29,30</sup> We compared the block developed during a train of pulses with that occurring during a single long pulse. The results of one experiment are illustrated in Figure 4. At all test potentials, substantially greater block developed during the single 2.15-second pulse compared with the train of 50-msec pulses. The block during the 2.15-second pulse was not strongly voltage dependent. Between  $-85$  and  $-60$  mV, the block increased from 77 to 89%. Therefore, in the case of lidocaine, the time spent at the depolarized potential appears to be an important element in the development of block. This is consistent with the slow time course for the development of block that we have demonstrated in the previous section and as reported by others.<sup>10–12</sup> The marked voltage dependence of block development during the pulse train reflects differences in the kinetics of block during the pulse and recovery during the interpulse interval. Block develops faster at more depolarized potentials, so pulses to these potentials should lead to greater block. The recovery potential and recovery interval was the same for all pulses. The data in Figure 4 also demonstrates that over a range of subthreshold potentials substantial block develops. Open channels are not necessary for block development.

### Block During Pulse Trains of Increasing Frequency

Frequency-dependent block of the sodium current during pulse-train stimulation has been analyzed for a simplified channel blockade model by Starmer and Grant<sup>31</sup> and Starmer et al.<sup>32</sup> If binding occurs predominately to a single class of binding site, a number of predictions follow directly from simple first-order binding kinetics. The rate of block development as measured by peak  $I_{Na}$  should follow

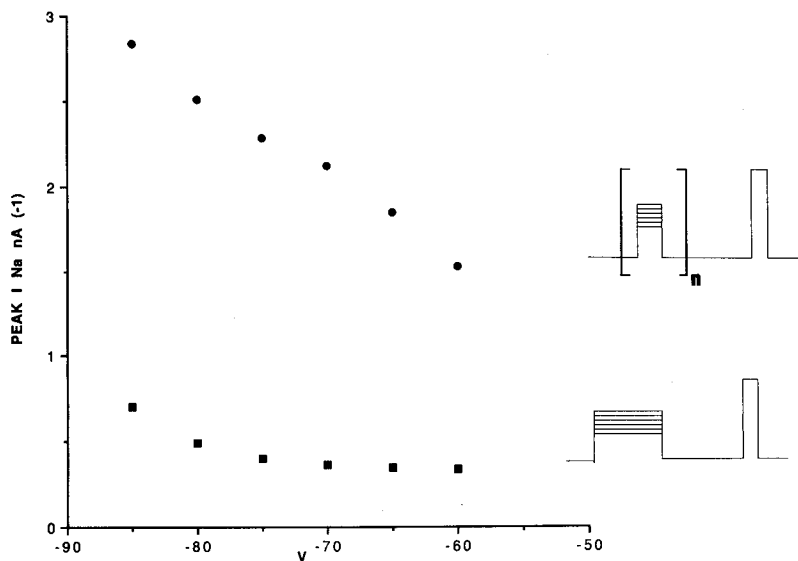


FIGURE 4. Plot showing a comparison of block of the sodium current produced by a train of pulses versus a single long pulse. A train of fifteen 50-msec pulses with interpulse intervals of 100 msec were applied to various potentials. A recovery interval of 500 msec was followed by a test to  $-20$  mV. The filled circles show the current during the test pulse. This was compared with the currents observed after a single 2.15-second pulse, a recovery interval of 500 msec, and test to  $-20$  mV (filled squares). In the absence of drug, the current at  $-20$  mV was  $-3.1$  nA. The data shown was obtained in  $80$   $\mu$ M lidocaine. The voltage pulse paradigms are summarized in the inset,  $n=15$ .

a single exponential at each interstimulus interval. The rate constants for the development of block should be directly related to the interstimulus interval, and the steady-state level of block should be inversely related to the interstimulus interval. There is a direct parallel between the exponential block developing during a single continuous pulse and the piecewise exponential block developing during a train of pulses.<sup>32</sup> Prior tests of the scheme in cardiac muscle have been performed with indirect measures of available sodium current such as  $V_{max}$ .<sup>33</sup> Therefore, we studied the rates of development of block during trains of pulses to  $-20$  mV at six different interstimulus intervals.

Figure 5 shows a composite of the decline in sodium current at these interstimulus intervals. Quantitative analysis required that a steady-state level of block be attained during the pulse train at all test cycle lengths. After trials of pulse trains of 10, 15, and 20 pulses, we observed that about 20

pulses were required to reach steady state at some cycle lengths. Therefore, we used trains of 25 pulses. At each interstimulus interval, block development could be described by a single exponential. Block developed faster as the interstimulus interval grew longer. As shown in panel A of Figure 6, there was a linear relation between the rate of development of block and the interstimulus interval. The steady-state level of block was also linearly related to a function of the interstimulus interval (Figure 6B).

The blocking effects during trains of pulses may be related to that during single pulses. The comparison may be useful, as in applied situations, where estimates based on pulse-train stimulation may facilitate obtaining binding parameters. To a first approximation, change in block during a cycle of the train can be viewed as consisting of net drug uptake during the pulse (duration ( $t_i$ )=50 msec) with a rate constant  $\lambda_i$ ; this is followed by partial recovery during the inter-

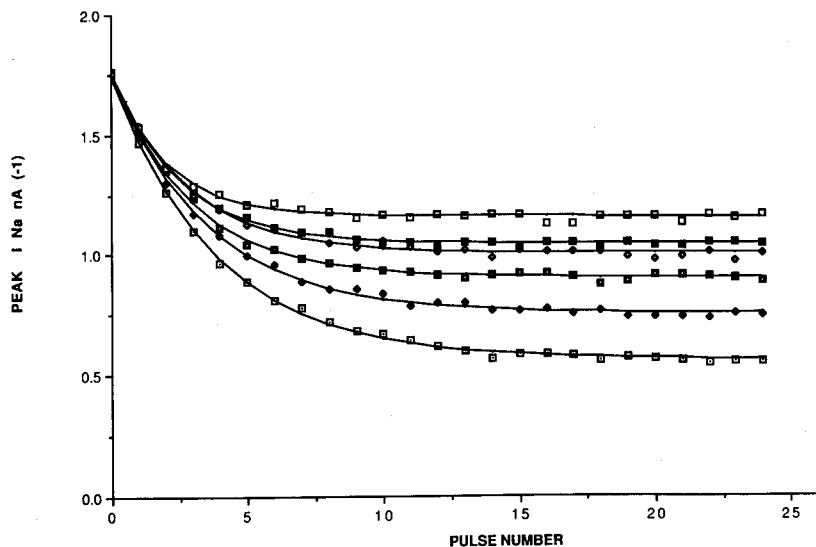


FIGURE 5. Plot showing decline of sodium current during pulse trains of various interstimulus intervals. The sodium current during trains of 50-msec pulses at interpulse intervals of 150 ( $\square$ ), 250 ( $\blacklozenge$ ), 350 ( $\blacksquare$ ), 450 ( $\blacklozenge$ ), 550 ( $\blacksquare$ ), and 650 msec ( $\square$ ) are plotted on the ordinate. The sequence of the pulse within the train is plotted on the abscissa. The continuous lines are least-squares fit to the data points of each pulse interval with a single exponential. The data were obtained in the presence of  $80$   $\mu$ M lidocaine.

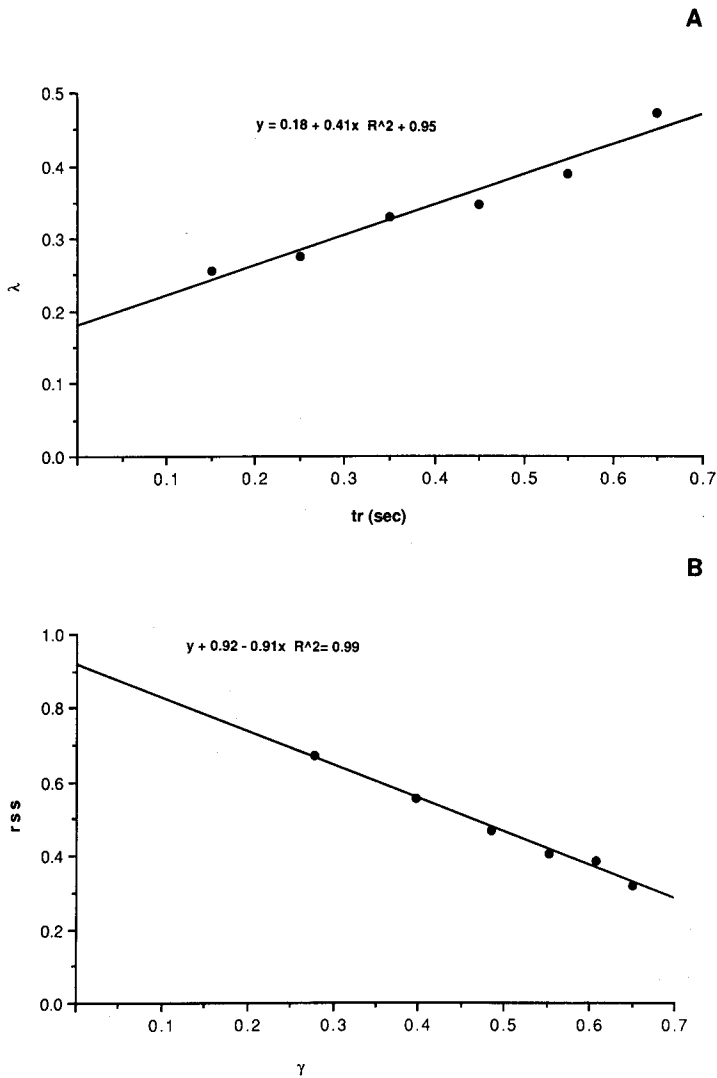


FIGURE 6. Graphs showing relations between the rate of development of block, the steady-state level of block, and the changing frequency of stimulation. In panel A, the rate constant for the development of block ( $\lambda$ ) at each interstimulus interval was obtained from the least-squares regression shown in Figure 5. These rate constants are plotted against the interpulse interval. The straight line is a least-squares fit to the point. The equation for the fit is shown with  $R^2=0.948$  (the square of the correlation co-efficient). In panel B, the steady-state level of block  $r_{ss}$  at each interpulse interval is plotted against  $\gamma$ , a variable defined in the text. The straight line is the least-squares fit to the data point. The equation for fit is shown with  $R^2=0.991$ .

pulse period duration  $t_r$  with rate constant  $\lambda_r$  at  $-120$  mV. At steady state, the increase in block during  $t_i$  is dissipated during the recovery period  $t_r$ .

It may be shown<sup>32</sup> that

$$r_n = r_{ss} - (r_o - r_{ss}) \exp(-n\lambda^*) \quad (8)$$

where  $r_n$  is degree of block at the end of the  $n$ th pulse,  $r_{ss}$  and  $r_o$  are constants, and  $\lambda^*$  is the uptake rate during the train.

$$\lambda^* = \lambda_i t_i + \lambda_r t_r \quad (9)$$

A plot of  $\lambda^*$  against  $t_r$  (150, 250, 350, 450, 550, and 650 msec for the pulse trains in Figure 6A) has  $\lambda_i t_i$  as intercept and  $\lambda_r$  as slope. The blocking rate during the pulse,  $\lambda_i$ , and the recovery rate constant at  $-120$  mV can be obtained. For the experiment illustrated in Figure 6  $\lambda_i = 3.6/\text{sec}$ , and  $\lambda_r = 0.41/\text{sec}$  (time constants of 0.277 and 2.4 seconds, respectively). The uptake rate determined with single pulses in the same cell was 2.3/seconds.  $\lambda_i$  obtained from pulse trains overestimates the rate of block development compared with that determined with the single pulse. This may be related to an element of activated-

state block during each pulse of the train. A small element of activated state block would be repeated 24 times during the train of pulses and could substantially enhance the rate of block during the trains of pulses compared with that during a single long pulse.

It can be shown that the fraction of blocked channels at steady-state,  $r_{ss}$ , is

$$r_{ss} = a_\infty + \gamma(r_\infty - a_\infty) \quad (10)$$

where  $\gamma = [1 - \exp(-\lambda_r t_r)] / [1 - \exp(-\lambda^*)]$ ,  $a_\infty$  is the equilibrium level of block for single pulse and  $r_\infty$  is the tonic level of block.  $\lambda_r$ ,  $t_r$ , and  $\lambda^*$  can be obtained from equation 10. From a plot of  $r_{ss}$  against  $\gamma$  (Figure 6B),  $a_\infty$  and  $r_\infty$  can be obtained. The equilibrium level of tonic block obtained from these calculations was 0.5% while the depolarized equilibrium was 92%.

We examined the issue of activated-state block by applying trains of 2-msec pulses at interpulse intervals of 150, 350, and 550 msec. As illustrated in Figure 7, substantial frequency-dependent block develops with these very brief pulses. This sug-

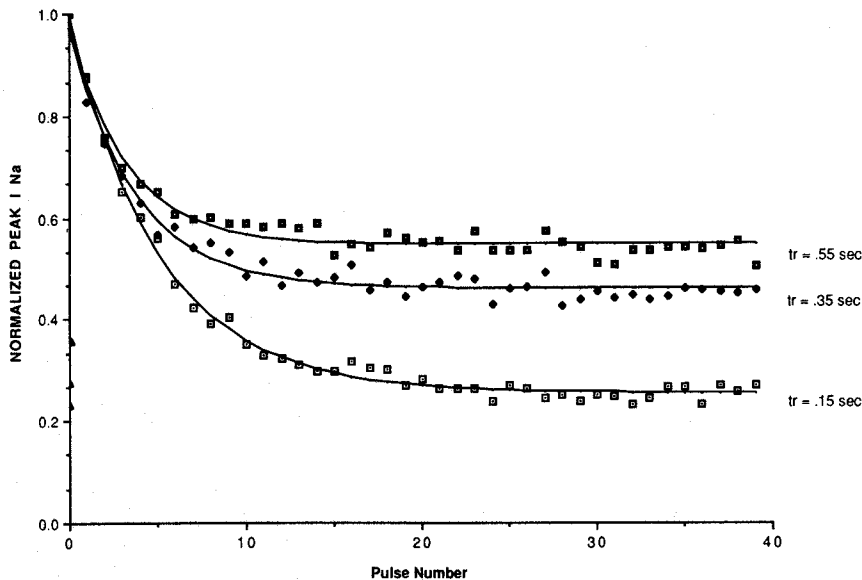


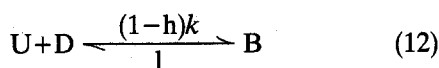
FIGURE 7. Graph showing use-dependent inhibition of the sodium current by trains of 2-msec pulses. The normalized peak sodium during trains at interpulse intervals ( $t_r$ ) of 150, 350, and 550 msec is plotted on the ordinate. The peak value of the current used for normalization was  $-4.0$  nA. The sequence of the pulse within the train is plotted on the abscissa. The figure shows that significant block develops with pulses as brief as 2 msec during lidocaine exposure.

gests that a more complicated scheme is required to describe block during pulse trains. A rate constant  $\lambda_a$  describing block during an activated state (duration  $t_a$ ) must be included. Equation 9 becomes:

$$\lambda^* = \lambda_a t_a + \lambda_i t_i + \lambda_r t_r \quad (11)$$

Definition of each component requires a series of experiments in which two of the three time intervals are changed. We make the simplifying assumption that changes in pulse duration from 10 to 50 msec do not change the component of activated-state block. Then, as the recovery interval is varied, the uptake rate ( $\lambda^*$ ) should remain a linear function of both the clamp interval ( $t_i$ ) and the recovery interval ( $t_r$ ). The relation can be visualized with two plots: one where  $t_i$  is held constant and  $t_r$  is varied and the other where  $t_r$  is held constant and  $t_i$  is varied. The slope of the first relation should give  $\lambda_r$  (Figure 8A). Similarly, as the clamp duration ( $t_c$ ) is varied beyond 10 msec,  $\lambda^*$  should be a linear function of clamp duration with slope equal to uptake rate  $\lambda_i$ . The results in figure 8B show that this is approximately the case.

When channel blockage appears voltage dependent, then apparent channel inactivation,  $h^*$ , as assessed by the two pulse protocols is obligated to shift in the hyperpolarizing direction. Since inactivation is measured in terms of available peak currents, then  $h^* = h(1-b)$ , where  $b$  is the apparent voltage sensitive fraction of blocked channels. We use the term voltage-sensitive block without inferring mechanisms. It could be due to an interaction between membrane field and drug charge or due to voltage-sensitive channel conformation transition rates. The amount of shift in the midpoint of the inactivation curve for lidocaine binding described by:



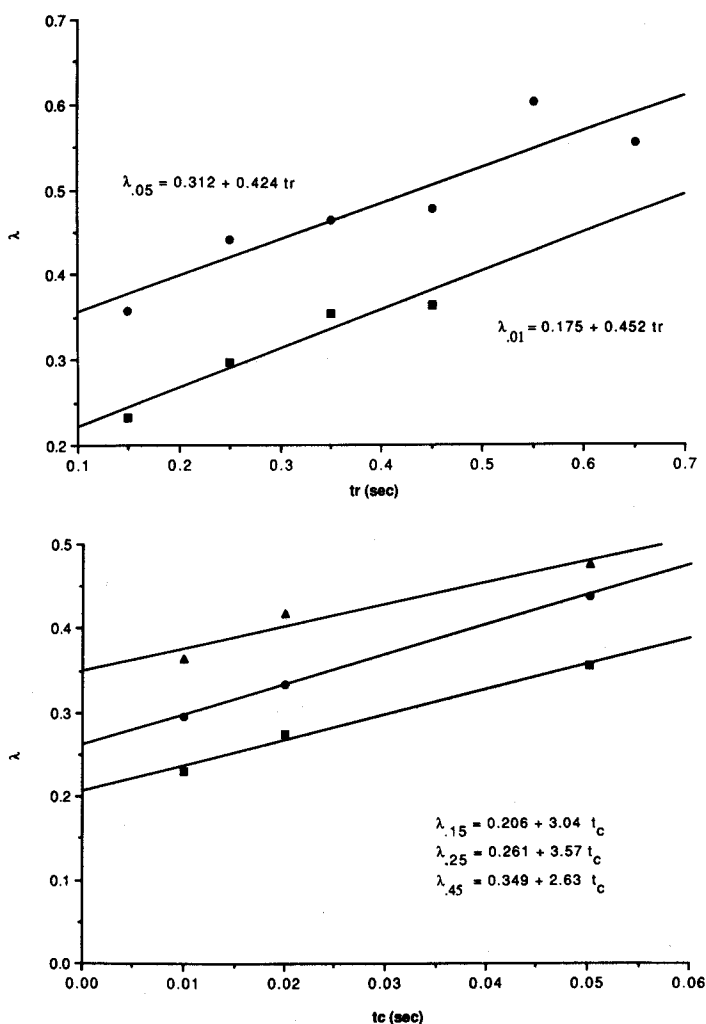
is given by<sup>34</sup>:  $\Delta V = s \times \ln(1 + kD/l)$ , where  $s$  is the slope factor for normal inactivation as described in the Boltzmann equation ( $h = 1/[1 + \exp(V - V_h)/s]$ ),  $kD$  is the forward blocking rate, and  $U$  and  $B$  are unblocked and blocked channels, respectively. We retain the voltage dependence in the form  $(1-h)$  despite our earlier results suggesting that the blocked state and the inactivated state may not be identical.  $l$  is the reverse rate constant.

The data from Figures 5 and 6 and for the continuous uptake rate at  $-20$  mV determined in the same cell yield values of  $kD = 2.08/\text{sec}$  and  $l = 0.234/\text{sec}$ . For this experiment the control slope factor was 5.9. The  $\Delta V$  calculated was 13.5 mV. For the frequency-dependent block with trains of stimuli,  $kD = 3.3/\text{sec}$ ,  $l = 0.29/\text{sec}$ , yielding a shift  $\Delta V = 14.9$  mV. The actual shift measured in this experiment was 16 mV. Thus voltage shifts determined from rates derived from the continuous block during a single pulse and those derived from pulse trains are similar and internally consistent with the observed shift in apparent inactivation.

## Discussion

### Measurement of the Sodium Current in Cultured Atrial Myocytes

We have studied the blocking action of lidocaine on the sodium current in cultured atrial myocytes. The cultured atrial myocyte proved to be a useful adult mammalian preparation to study the properties of the sodium current. It is not clear why the cells assume a spherical shape after 24 or more hours in culture. This change in morphology has been observed with other adult myocyte preparations.<sup>35</sup> The spherical shape was usually maintained for 5 or more days, unlike neonatal myocytes, which assume an elongated shape within 48 hours. Because of the small size of the cells, special procedures were not required to reduce the membrane area that had to be clamped (e.g., Reference



**A** FIGURE 8. Graphs showing kinetics of block during pulse-train stimulation when interpulse interval and pulse duration are both varied in the same cell.  $\lambda$ , rate constant for the development of block,  $t_c$ , clamp duration. We assume three components to the blocking process: 1) one component with uptake rate  $\lambda_a$  for a time interval  $t_a$ , which represents binding to an activated channel conformation, 2) a component with uptake rate  $\lambda_i$  during a time period  $t_i$ , which represents binding to some intermediate conformation with voltage dependence similar to but not identical with the inactivated state, and 3) a component with uptake rate  $\lambda_r$  during a time period  $t_r$ , which represents binding occurring at the resting potential. We do not specify the channel conformation to which binding is occurring. The entire uptake process ( $\lambda^*$ ) during the train can now be specified:  $\lambda^* = \lambda_a t_a + \lambda_i t_i + \lambda_r t_r$ .

**B** Panel A: Uptake rates as a function of recovery interval ( $tr$ ) for clamp durations of 10 (■) and 50 (●) msec. The above relation for  $\lambda^*$  predicts that the curve describing the kinetics for 10 and 50 msec should be parallel, but the intercept should be greater for the 50-msec pulse. This is borne out in the figure. Panel B: Uptake rates as a function of clamp interval for three different recovery intervals. Here, the theoretical intercept is  $\lambda_a \lambda_a + \lambda_r t_r$ , which predicts greater rates of block development for greater recovery intervals. The lines are consistent with these predictions. Multiple regression of the data in panels A and B yielded  $\lambda_a = 153 \pm 15/\text{sec}$ ,  $\lambda_i = 3 \pm 0.3/\text{sec}$  and  $\lambda_r = 0.42 \pm 0.05/\text{sec}$ . The rate of continuous uptake during single pulses in the same cell was  $2.9 \pm 0.1/\text{sec}$ , in agreement with  $\lambda_i$  estimated from the pulse trains.

36). The small cell size and geometry of the cells provided favorable conditions to voltage clamp the sodium current. Adequacy of voltage control is best demonstrated by introducing a second voltage-sensing electrode into the cell. This was not feasible in a 30- $\mu\text{m}$  cell. However, we used other criteria as a guide to adequacy of the voltage clamp. The current traces were free of notches, no threshold phenomena were observed in negative limb of the I-V curve, and there was no crossover of current traces as the magnitude of the current was varied by changing the holding potential. In 90% of trials, we were able to obtain an adequate voltage clamp. This was achieved in a relatively high external sodium concentration of 75 mM. However, it was necessary to lower the temperature to 15° C to obtain consistent separation of the capacitive transient and inward sodium current. The 50–150- $\mu\text{sec}$  duration of the capacitive transient without series resistance compensation compares very favorably with that obtained using two

microelectrodes or a single suction electrode in larger cells.<sup>12</sup>

The features of the sodium current were similar to those reported in other dialyzed cardiac cells (e.g., Reference 12). There was one important departure. Inactivation developed with a single exponential time course in both the subthreshold and threshold levels of membrane potential. Many studies report second-order development of inactivation.<sup>19,24,37</sup> However, in some studies, the magnitude of the smaller component was as low as 2%.<sup>37</sup> We doubt that such small components can be identified with certainty. Ebihara et al<sup>38</sup> and Fujii et al<sup>39</sup> reported single exponentials for the development of inactivation in spherical aggregates or single cultured chick embryonic cells.

#### Block With Single Pulses

The major results of the study are that lidocaine blocks the sodium current in both the subthreshold and suprathreshold ranges of membrane potential

with kinetics that are voltage dependent. The presence of block in the subthreshold range of membrane potential confirms earlier studies in frog node of Ranvier by Khodorov et al<sup>40</sup> and in cardiac muscle by Sanchez-Chapula et al<sup>12</sup> and Bean et al.<sup>11</sup> We are confident that the potential of  $-80$  mV is subthreshold in these cells. We have recorded up to 200 depolarizing steps of 200-msec duration in cell-attached patches in these cells at  $-80$  mV without observing a single event; these were readily apparent at  $-60$  mV or less (authors' unpublished observations). These are the best data we have available; they show that there is indeed a subthreshold level of potential. However, these data do not provide absolute proof for such a potential range. We only wish to make the point that openings are rare at  $-80$  mV, yet block is always observed at this potential with sufficiently long pulses during lidocaine exposure. The presence of subthreshold block is at variance with one of the assumptions used to explain lidocaine block by the guarded receptor model.<sup>14</sup> In this model, it was assumed that the activation parameter controlled access of drug to its receptor site. The effect of the membrane field on the blocking molecule and trapping of the drug by closing of the channel gate conferred further voltage dependence. These concepts require modification. To a first approximation, it appears as though a transition having voltage dependence similar to channel inactivation controls access of drug to a receptor site as block develops during prolonged pulses.<sup>40</sup> Indeed, it is not at all clear that the membrane gates as described in the Hodgkin-Huxley formalism control access of drug to its binding site or modulate binding of drug to its receptor.

An important result of this study relates to the kinetics of drug block during a single pulse. They are an extension of prior studies done using  $V_{\max}$  or direct  $I_{Na}$  measurements.<sup>7,11,12</sup> In the present study, we used a sufficient number of data points so that accurate estimates of the binding kinetics could be obtained. Blocking of the sodium channel is a slow process, with a time constant in the range of 350–900 msec. We were able to demonstrate two additional properties of the kinetics of block: 1) block developed with a single exponential time course, and 2) the kinetics of block were voltage dependent.

The assignment of one or two exponentials to a kinetic process is not trivial. Unfortunately, multiple exponential fits are often used without some test of significance. We used  $F$  statistics based on the sum of squared errors to estimate appropriate fits. At the level of 0.05, our data for block development were well fitted by a single exponential. As we have outlined in the results, a single exponential fit is generally not consistent with a binding scheme involving three sequential states. Estimates of what the faster exponential should be at  $-20$  mV indicate that it could readily be missed by the protocol that we used. At  $-80$  mV, the inactivation rate was

about one third of the overall blocking rate. An exponential component of this rate should have been resolvable. Khodorov et al<sup>40</sup> fit their blocking data to a single exponential. The range of potentials extended from  $-113$  to  $-37$  mV. This covers potentials more negative than the current study. The onset of inactivation would be slower at these potentials, and a true delay should have been evident. They observed blocking time constants of 50–400 msec at room temperature. The data in Tables 1 and 5 of their study suggest that the blocking time constant approaches a limiting value above threshold. A limiting value for the blocking time constant would be consistent with a relatively rapid voltage-independent inactivation process above threshold and also voltage-independent blocking. In heart muscle, Sanchez-Chapula et al<sup>12</sup> reported the blocking action of  $20 \mu\text{M}$  lidocaine during single pulses at  $-30$  mV at room temperature. They found a mean blocking half-time of 115 msec (corresponding time constant 166 msec) in three experiments. Considering the differences in temperature at which the experiments were performed, this value is consistent with the values we observed. They also reported more strongly voltage-dependent block in the subthreshold range of potentials (compare their Figure 9B with our Figure 4). We think that the difference relates to the duration of the pulse chosen to demonstrate block. The 500-msec pulse that they used was not sufficient to reach steady state at the potentials tested. We used pulses of 2.15 seconds.

The rate of development of block by lidocaine has been examined in two other cardiac preparations. In the study of Bean et al,<sup>11</sup> block developed at similar rates at  $-69$  and  $+30$  mV in the presence of lidocaine. Only when the pH was increased to 8.5 and the lidocaine concentration was increased to  $200 \mu\text{M}$  was more rapid onset of block noted at  $-40$  mV compared with  $-60$  mV. Actual kinetic parameters for the blocking process were not provided. Matsubara et al<sup>7</sup> used  $V_{\max}$  measurements to determine the rate of development of block during exposure to  $5$ – $40 \mu\text{M}$  lidocaine. They showed that block developed "exponentially" but was voltage independent over a voltage range of  $-40$  to  $+40$  mV. Their experiments were performed at  $37^\circ\text{C}$ . The voltage independence of block that they observed is different from that reported here. Although a non-linearity between  $V_{\max}$  and available sodium conductance<sup>41</sup>  $g_{Na}$  may account for the differences between our study and that of Matsubara et al,<sup>7</sup> this could not account for the apparent differences in the results of Bean et al.<sup>11</sup>

The present study provides more detailed analysis of block development with the direct  $I_{Na}$  measurements than previous studies in cardiac preparations. The single exponential time course of block development that we observed is more consistent with simple voltage dependence of block than the sequential scheme 1. Calculations of the two rate constants for the development of block would

involve further assumptions about the voltage dependence of the rate constant  $k_2D$  in Equation 7. A scheme similar to 1, but having very rapid transitions into a bindable state at all voltages, could account for the results. This channel conformation would have voltage dependence similar to traditional inactivation. We recognize that any analysis such as the one we have done involves simplifications. For example, we have assumed a single blocking drug species. At pH 7.4, lidocaine exists in both the charged and the uncharged forms. However, in the subthreshold range of membrane potential, the available data are consistent with the uncharged form as the only blocking species in the subthreshold range of potentials.<sup>13</sup> Our observations could be extended by performing experiments with predominantly neutral or charged drug forms and extending the range of potential studies to those in which the inactivation process shows little voltage dependence.

The strongest evidence linking the development of block and the inactivated state are those experiments performed with inactivation removed. Cahalan<sup>42</sup> examined the blocking action of eight compounds in pronase-treated squid giant axons. Lidocaine was not studied. However, the structurally similar analogue etidocaine retained partial use-dependent block whereas the analogues QX314 lost their use-dependent effects. A brief communication by Zaborovskaya and Khodorov<sup>43</sup> suggests that lidocaine did not induce slow sodium channel inactivation following a chloramine-T treatment. However, supporting data were not presented. All the treatments used to remove sodium inactivation are fairly drastic and cause effects other than removal of inactivation, for example, a substantial fall in conductance.<sup>44-46</sup> The possibility certainly exists that these treatments may modify or abolish drug binding to a receptor that is not identical to the inactivated state.

#### *Block During Pulse Train Stimulation*

Our experiments show that much greater block develops during single prolonged pulses that form the envelope for a train of pulses. The train of pulses contain a 100-msec recovery interval between pulses. The voltage-time integral is therefore 35% of that during the single pulse. This suggests that time spent at the depolarized potential is a major factor for blockade development. These results differ from those of Matsubara et al.<sup>7</sup> They showed much greater decrease of  $V_{\max}$  during trains of 5-msec pulses to +20 mV than with single pulses, provided the number of pulses in the train was less than about 35 (Figure V of Matsubara et al<sup>7</sup>). The experimental conditions are sufficiently different: temperature of 37° C versus 15° C, sodium concentration of 143 mM versus 75 mM, test potential of +20 versus less than -60 mV, and  $V_{\max}$  versus  $I_{Na}$  measurement. Because of these experimental variations, little interpretation can be placed on the observed differences.

A preliminary result from their group using  $I_{Na}$  measurements in voltage-clamped atrial myocytes suggests that the test voltage may be critical (Figure 2 of Hondeghem<sup>47</sup>). It would be of interest to see if the level of block produced by the two-pulse paradigms in Figure 4 converges at strongly depolarized potentials ( $\sim +20$  mV).

We have examined the block produced by lidocaine during pulse-train stimulation as a function of the interval between pulses. The procedure is potentially very useful because theoretical analysis suggests that binding parameters of drugs to its receptor site may be so obtained.<sup>33</sup> The response to pulse-train stimulation may be readily applied to the in situ heart in experimental animals and in humans. For example, it is neither practical nor in some cases possible to use the long recovery periods required to measure recovery kinetics in the in situ heart. The decline of peak  $I_{Na}$  during pulse-train stimulation was well fitted by a single exponential for interpulse intervals of 150-650 msec. These results are consistent with those of Bean et al,<sup>11</sup> who also observed a single exponential decline. The rate constant for the decline of  $I_{Na}$  was a linear function of the interpulse interval. This is consistent with a theory that assumes binding to one site. However, the blocking rate that we observed with pulse train stimulation was greater than that with a single prolonged pulse. This may be related to an element of activated state blockade at -20 mV.<sup>47</sup> Finally, sodium-channel availability measured in the presence of 80  $\mu$ M lidocaine  $h^*$  was found shifted by 16 mV in the hyperpolarizing direction. Since availability is based on the peak current, then in the presence of drug, it reflects  $h$ , in the fraction of unblocked channels ( $1-b$ ), that is,  $h^*=h(1-b)$ . Since block exhibits an apparent voltage dependence, then  $h$  will not be scaled by the same amount at each voltage, resulting in an obligatory hyperpolarizing shift in midpoint. For the binding scheme<sup>11</sup> the obligating shift is:

$$\Delta V = s \times \ln(1 + kD/l)$$

From the binding parameters obtained during the single pulse and the pulse train protocol, we calculated the shift in the apparent inactivation curve. The observed shift was 1-3 mV greater than the predicted shift. The time-dependent shift in the  $h_{\infty}$  curve could account for the discrepancy. Thus, interpretation of shifts in channel availability must be done with care, after first adjusting for the shift expected from blockade.

In summary, we have observed block of cardiac sodium channels by lidocaine in both the subthreshold and threshold ranges of membrane potential. The final level of block is consistent with lidocaine binding to a channel conformation having similar voltage dependence to the inactivated state. However at subthreshold testing potentials where the development of inactivation is slow, we did not observe a second-order delay in the development of

blockade. This suggests binding to a channel conformation having a similar voltage dependence to the inactivated state but having rapid voltage-dependent equilibration.

### Acknowledgments

We would like to acknowledge the technical support of Ms. Anne Stone. We express our gratitude to Ms. Pat Dean for preparing the manuscript and Dr. K. Lee of the section of Clinical Epidemiology at Duke University for helping with the statistical analysis. Some of the programs used in this study were provided by the National Biomedical Simulation Resource.

### References

- Hondeghem LM, Katzung BG: Antiarrhythmic agents: The modulated receptor mechanism of action of sodium and calcium channel-blocking drugs. *Annu Rev Pharmacol Toxicol* 1984;24:387-423
- Grant AO, Starmer CF, Strauss HC: Antiarrhythmic drug action blockade of the inward sodium current. *Circ Res* 1984;55:427-439
- Davis LD, Temte JV: Electrophysiological action of lidocaine on ventricular muscle and Purkinje fibers. *Circ Res* 1969;24:639-655
- Grant AO, Strauss LJ, Wallace AG, Strauss HC: The influence of pH on the electrophysiological effects of lidocaine in guinea-pig ventricular myocardium. *Circ Res* 1980;47:542-550
- Oshita O, Sada H, Kojima M, Ban T: Effects of tocainide and lidocaine on the transmembrane action potentials as related to external potassium and calcium concentrations in guinea-pig papillary muscles. *Naunyn Schmiedebergs Arch Pharmacol* 1980;314:67-82
- Chen CM, Gettes LS, Katzung BG: Effect of lidocaine and quinidine on steady-state characteristics and recovery kinetics of  $dV/dt_{max}$  in guinea-pig ventricular myocardium. *Circ Res* 1975;37:20-29
- Matsubara T, Clarkson C, Hondeghem LM: Lidocaine blocks open and inactivated cardiac sodium channels. *Naunyn Schmiedebergs Arch Pharmacol* 1987;336:224-231
- Kojima M, Ban T: Nicorandil shortens action potential duration and antagonises the reduction of  $V_{max}$  by lidocaine but not disopyramide in guinea pig papillary muscles. *Naunyn Schmiedebergs Arch Pharmacol* 1988;337:203-212
- Weld FM, Bigger JT Jr: Effects of lidocaine on the early inward transient current in sheep cardiac Purkinje fibers. *Circ Res* 1975;37:630-639
- Hondeghem LM, Katzung BG: Time- and voltage-dependent interactions of antiarrhythmic drugs with cardiac sodium channels. *Biochim Biophys Acta* 1977;472:373-398
- Bean BP, Cohen CJ, Tsien RW: Lidocaine block of cardiac sodium channels. *J Gen Physiol* 1983;81:613-642
- Sanchez-Chapula J, Tsuda Y, Josephson IR: Voltage- and use-dependent effects of lidocaine on sodium current in rat single ventricular cells. *Circ Res* 1983;52:557-565
- Hille B: Local anesthetics: Hydrophilic and hydrophobic pathways for drug-receptor reaction. *J Gen Physiol* 1977;69:497-515
- Starmer CF, Grant AO, Strauss HC: Mechanism of use-dependent block of sodium channels in excitable membranes by local anesthetics. *Biophys J* 1984;46:15-27
- Starmer CF, Grant AO: Phasic ion channel blockade: A kinetic and parameter estimation procedure. *Mol Pharmacol* 1985;28:347-356
- Starmer CF, Courtney KR: Modelling ion channel blockade at guarded sites: Application to tertiary drugs. *Am J Physiol* 1986;251:H848-H856
- Colatsky TJ: Voltage clamp measurements of sodium channel properties in rabbit cardiac Purkinje fibers. *J Physiol (Lond)* 1980;305:215-234
- Makielski JC, Sheets MF, January CT, Fozzard HA: Can sodium channels inactivate without first activating in cardiac Purkinje cells (abstract)? *J Gen Physiol* 1985;86:12a
- Follmer CH, Ten Eick RE, Yeh JZ: Sodium current kinetics in cat atrial myocytes. *J Physiol (Lond)* 1987;384:169-197
- Grant AO, Starmer CF: Mechanism of closure of cardiac sodium channels in rabbit ventricular myocytes: Single-channel analysis. *Circ Res* 1987;60:897-913
- Bechem M, Pott L, Rennebaum H: Atrial muscle cells from hearts of adult guinea-pigs in culture: A new preparation for cardiac cellular electrophysiology. *Eur J Cell Biol* 1983;31:366-369
- Hamill OP, Marty A, Neher E, Sakmann B, Sigworth F: Improved patch-clamp techniques for high-resolution current recording from cell and cell-free membrane patches. *Pflügers Arch* 1981;391:85-100
- Marquardt DW: An algorithm for least-squares estimation of non-linear parameters. *J Soc Ind Appl Math* 1963;11:431-441
- Clark RB, Giles W: Sodium current in single cells from bullfrog atrium: Voltage dependence and ion transfer properties. *J Physiol (Lond)* 1987;391:235-265
- Becham M, Pieper F, Pott L: Guinea-pig atrial cardioball. *Basic Res Cardiol* 1985;80(suppl 1):19-25
- Brown AM, Lee KS, Powell T: Sodium current in single rat heart muscle cells. *J Physiol (Lond)* 1981;318:479-500
- Aldrich RW, Stevens CF: Inactivation of open and closed sodium channels determined separately. *Symposia on Quantitative Biology* 1983;47:147-153
- Gilbert DL, Lipicky RJ: A model of drug-channel interaction in squid axon membrane, in Adelman WJ, Goldman PE (eds): *The Biophysical Approach to Excitable Systems*. New York, Plenum Publishing Corp, 1981, pp 213-251
- Colatsky TJ: Action of local anesthetics and antiarrhythmics on membrane channels in the heart, in Covina BG, Fozzard HA, Rehder K, Strichartz G (eds): *Effects of Anesthesia*. Bethesda, Md, American Physiological Society, 1985, pp 65-73
- Hondeghem LM, Matsubara T: Quinidine blocks cardiac sodium channels during opening and slow inactivation in guinea-pig papillary muscle. *Br J Pharmacol* 1988;93:311-318
- Starmer CF, Grant AO: Phasic ion channel blockade: A kinetic model and parameter estimation procedure. *Mol Pharmacol* 1985;28:345-356
- Starmer CF, Packer DL, Grant AO: Ligand binding to transiently accessible sites: Mechanism for varying apparent binding rates. *J Theor Biol* 1987;124:335-341
- Packer DL, Grant AO, Strauss HC, Starmer CF: Determination of apparent binding affinities from use-dependent conduction delay and  $V_{max}$  reduction in Purkinje fibers. *Circulation* 1986;74:2-20
- Starmer CF, Nesterenko VV, Undrovinas IA, Packer DL, Gilliam FR III, Grant AO, Rosenstraukh LV, Strauss HC: Characterizing ion channel blockade with the guarded receptor hypothesis, in Hondeghem LM (ed): *Proceedings on Antiarrhythmic Drugs*. Nashville, Vanderbilt University, 1988
- Jacobson SL, Banfalvi M, Schwarzfled FA: Long-term primary cultures of adult human and rat cardiomyocytes. *Basic Res Cardiol* 1985;80(suppl 1):79-82
- Makielski JC, Sheets MF, Hanck DA, January CT, Fozzard HA: Sodium current in voltage clamped internally perfused canine cardiac Purkinje cells. *Biophys J* 1987;52:1-11
- Benndorf K, Nilius B: Inactivation of sodium channels in isolated myocardial mouse cells. *Eur Biophys J* 1987;15:117-127
- Ebihara L, Shigetom M, Lieherman M, Johnson EA: The initial inward current in spherical clusters of chick embryonic heart cells. *J Gen Physiol* 1980;75:437-456
- Fujii S, Ayer RK Jr, DeHaan RL: Development of the fast sodium current in early embryonic chick heart cells. *J Membr Biol* 1988;101:209-223



40. Khodorov B, Shishkova L, Peganov E, Revenko S: Inhibition of sodium currents in frog Ranvier node treated with local anesthetics. Role of slow sodium inactivation. *Biochim Biophys Acta* 1976;433:409-435
41. Cohen CJ, Bean BP, Tsien RW: Maximum upstroke velocity as an index of available sodium conductance. *Circ Res* 1984; 54:636-651
42. Cahalan MD: Local anesthetic block of sodium channels in normal and pronase-treated squid giant axons. *Biophys J* 1978;23:285-311
43. Zaborovskaya LD, Khodorov BI: The role of inactivation in the cumulative blockade of voltage-dependent sodium channels by local anesthetics and antiarrhythmics. *Gen Physiol Biophys* 1984;3:517-520
44. Brodwick MS, Eaton DC: Sodium channel inactivation in squid axon is removed by high internal pH or tyrosine-specific reagents. *Science* 1978;200:1494-1496
45. Nonner W, Spalding BC, Hille B: Low intracellular pH and chemical agents slow inactivation gating in sodium channels of muscle. *Nature* 1980;284:360-363
46. Rack M, Rubly N, Waschow C: Effects of some chemical reagents on sodium current inactivation in myelinated nerve fibers of the frog. *Biophys J* 1986;50:557-564
47. Hondeghem LM: Antiarrhythmic agents: Modulated receptor applications. *Circulation* 1987;75:514-520

---

KEY WORDS • sodium current • lidocaine • sodium-channel inactivation